The Astrophysical Journal Letters, 738:L27 (5pp), 2011 September 10 doi:10.1088/2041-8205/738/2/L27

SUPERNOVA SHOCK-WAVE-INDUCED CO-FORMATION OF GLASSY CARBON AND NANODIAMOND

Rhonda M. Stroud[1], Matthew F. Chisholm[2], Philipp R. Heck[3,4], Conel M. O'D. Alexander[5], and Larry R. Nittler[5]
[1] Materials Science and Technology Division, Naval Research Laboratory, Washington, DC 20375-0001, USA
[2] Materials Science and Technology Division, Oak Ridge National Laboratory, Oak Ridge, Tennessee, TN 37831-6069, USA
[3] Robert A. Pritzker Center for Meteoritics and Polar Studies, The Field Museum, Chicago, Illinois, IL 60605-2496, USA
[4] Chicago Center for Cosmochemistry, University of Chicago, Illinois, IL 60637-1433, USA
[5] Department of Terrestrial Magnetism, Carnegie Institution of Washington, Washington, DC 20015-1305, USA
Received 2011 June 27; accepted 2011 July 26; published 2011 August 23

ABSTRACT

Nanodiamond (ND) was the first extrasolar dust phase to be identified in meteorites. However, the 2 nm average size of the NDs precludes isotopic analysis of individual particles, and thus their origin(s) remains controversial. Using electron microscopy with subnanometer resolution, we show that ND separates from the Allende and Murchison meteorites are actually a two-phase mixture of ND and glassy carbon. This phase mixture is likely the product of supernova shock-wave transformation of pre-formed organics in the interstellar medium (ISM). The glassy carbon–ND mixture is also a plausible contributor to the 2175 Å extinction feature in the diffuse ISM.

Key words: astrochemistry – dust, extinction – meteorites, meteors, meteoroids – shock waves

1. INTRODUCTION

Lewis et al. (1987) first showed that nanodiamond (ND) isolated from primitive, carbonaceous meteorites carried Xe isotope anomalies indicative of an extrasolar origin. The large isotope anomalies in Xe isotopes, and smaller anomalies in Te (Richter et al. 1998), Pd (Maas et al. 2001), and Ba (Lewis et al. 1991) observed in bulk analyses of ND separates can be only explained by nucleosynthetic processes in supernovae. Noble gas release profiles from ion-implanted synthetic ND reproduce those of the meteoritic NDs, adding support to the idea of extrasolar ND formation (Huss et al. 2008). However, based on the abundances of the noble gases, e.g., 1 Xe atom per 10^5 NDs, and bulk C and N isotope compositions of the ND separates that are within the range of solar values, only a minor component of the separates is required to have originated in supernovae. Multiple spectroscopic studies (Bernatowicz et al. 1990; Blake et al. 1988; Hill et al. 1997; Lewis et al. 1987) of these separates suggest that up to 50% of the C is present in non-diamond form, although this has been attributed to surface reconstruction of the NDs (Garvie 2006) and contamination with terrestrial C. In the absence of isotopic measurements from individual NDs, which are not yet technically feasible, multiple origins for the NDs have been proposed, including condensation in the interstellar medium (ISM), the outflows of supernovae (Clayton 1989; Daulton et al. 1996) and Red Giant stars (Alexander 1997; Verchovsky et al. 2006), and in the solar nebula (Dai et al. 2002).

Astronomical observations of diamond in circumstellar and protoplanetary disk settings have a similarly long and controversial history because of the lack of a unique IR feature indigenous to diamond (Acke & van den Ancker 2006). Most observations have been inferred on the basis of plausible surface termination species, e.g., 3.43 μm and 3.53 μm C–H stretch bands (Guillois et al. 1999), which are also features of polycyclic aromatic hydrocarbons (PAHs; Petrie et al. 2003). Laboratory determination of the atomic-scale structure of meteoritic NDs could aid in the interpretation of the observed IR spectra, through identification of relevant surface terminations or optically active impurities.

Although it is not yet feasible to measure the isotopic compositions of individual 2 nm diamonds, aberration-corrected scanning transmission electron microscopy (STEM) now permits imaging and speciation of individual atoms down to B or below (Krivanek et al. 2010). In light of this recent advance, we sought to re-address the question of the location of the noble gas atoms in the ND separates, the origin of the non-diamond spectroscopic feature, and whether these properties indicate a specific astrophysical origin for the diamonds.

2. METHODS

We used aberration-corrected annular dark-field imaging and electron energy loss spectroscopy (EELS) at 60 kV, and conventional bright-field (BF) TEM imaging at 200 kV, to characterize acid-resistant separates from the Murchison and Allende meteorites. The Allende sample is an aliquot of the Allende DM separate prepared by Lewis et al. (1987); the Murchison separate was produced using a similar protocol, except that for the first step CsF–HCl was used instead of HF–HCl. Both protocols result in complete removal of any graphite or organic C. To minimize the chance of contamination with terrestrial C and also to optimize imaging conditions, measurements were performed on 5 nm thick, C-free, amorphous Si support films, which were first cleaned with an argon plasma, as well as on lacey C and 3 nm C-backed lacey C support films. Aliquots of the Allende DM and Murchison separates suspended in ultrahigh purity water were drop cast onto each of the types of support films. Prepared samples were stored between dimpled glass slides that were first baked at 160°C overnight.

BF and high-resolution (HR) TEM of the Allende DM and Murchison samples were performed at the Naval Research Laboratory with a JEOL 2200 field emission microscope. Aberration-corrected STEM was performed at Oak Ridge National Laboratory with a Nion UltraSTEM 100, equipped with an Enfina electron energy loss spectrometer. High- and medium-angle annular dark-field (HAADF and MAADF) imaging and EELS were performed at an operating voltage of 60 kV. Samples on all three type of support film were examined. The lowest background low-loss and C K-edge EELS spectra were obtained for samples supported on lacey C. Although single-phase measurements could not be obtained from the agglomerates that extended over the large holes in these films, the phases could be spatially resolved over the smallest holes

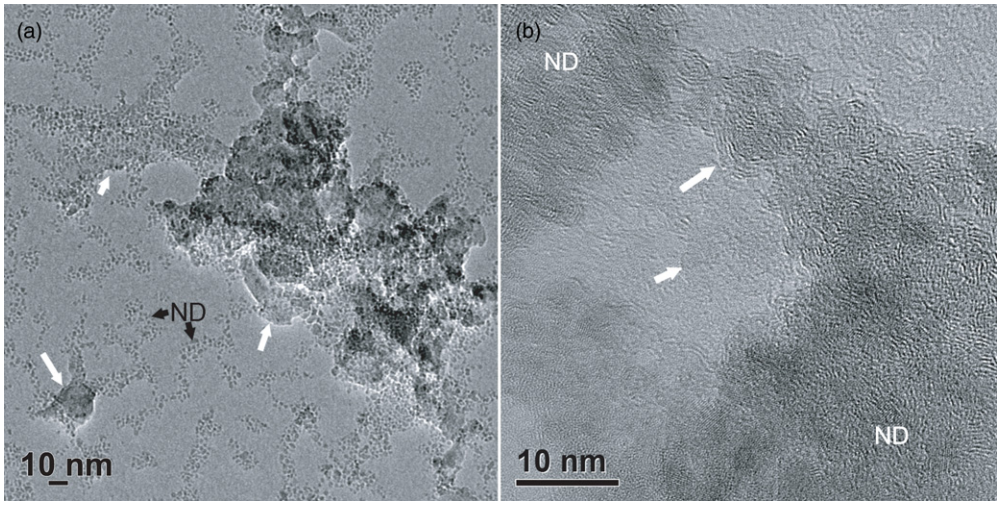

Figure 1. (a) Bright-field TEM image of a nanodiamond separate from the Murchison meteorite, supported on a 5 nm thick amorphous Si membrane. White arrows indicate areas of disordered C. ND refers to nanodiamonds. (b) Bright-field TEM images of the Allende DM nanodiamond separate on a 3 nm C support.

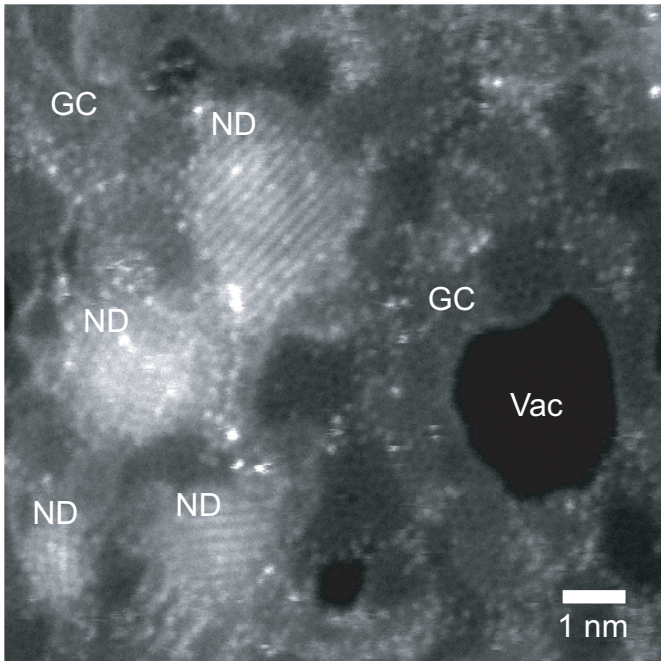

Figure 2. MAADF STEM image of the Murchison nanodiamond separate. Four nanodiamonds are shown (ND) surrounded by disordered C with a random packing of 5, 6, and 7 member rings (GC). Individual impurity atoms appear as isolated bright spots. The label Vac refers to vacuum regions of the image.

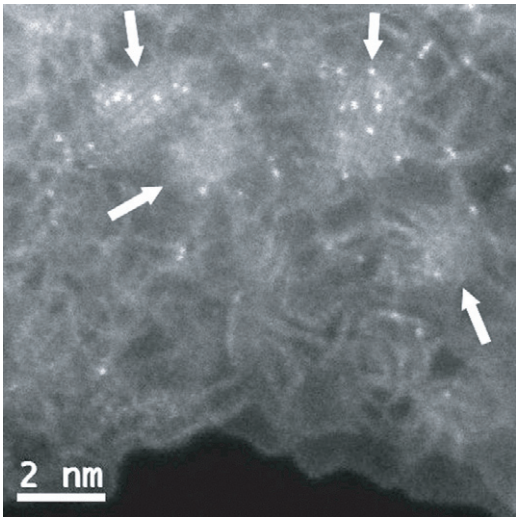

Figure 3. MAADF STEM image of the Allende DM separate. The white arrows indicate four nanodiamonds. Disordered C with a wrinkled-sheet appearance spans the space between diamonds. White spots are individual impurity atoms.

(<50 nm), which were spanned by a monolayer of diamonds connected by a disordered C phase. This permitted spectra to be obtained that were free from any contribution from the support film. To ensure the representative nature of the spectra, multiple spectra were collected from multiple regions of each separate. The low-loss spectra were processed to remove the zero-loss peak by the single-scattering deconvolution method, and the spectra were normalized to the total integrated intensity.

3. RESULTS

Non-crystalline, disordered carbonaceous material, in addition to ND, is clearly visible in the conventional BF image of the Murchison separate on the Si support film (Figure 1(a)). Similar disordered material was also observed in TEM images of the Allende separate on 3 nm thick C support films (Figure 1(b)). This disordered C covers the support film and coats the NDs, in some cases giving the appearance of an onion-like surface to the particles. However, when supported on traditional 25 nm thick lacey C, the disordered C is not readily apparent in BF TEM images, due to insufficient contrast. Although the disordered C wets the NDs and the C support film, it is not self-supporting over large holes in the film, where monolayer variations in C thickness could be distinguished.

MAADF STEM imaging of the Murchison (Figure 2) and Allende (Figure 3) separates reveals the ND (111) planes, sheet-like C with a disordered ring structure, and individual impurity atoms. The STEM probe size for these measurements is estimated to be 150 pm; smaller than the diameter of a six-member C ring, but larger than the C–C bond distance (∼142 pm). Local variation in the dimensions and packing of the C rings is visible, although the individual C atoms are not resolved. The STEM images show that the NDs do not have onion-like surface structures, and that this appearance in the lower-resolution TEM images was due to the second phase.

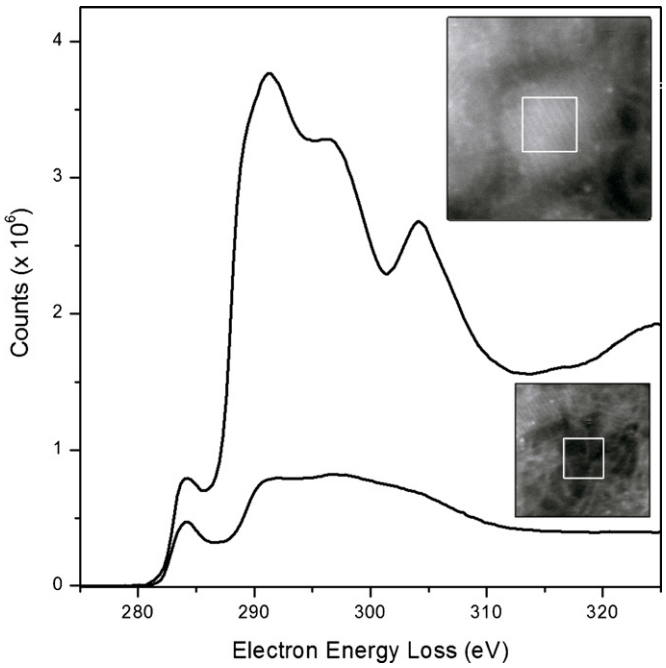

Figure 4. Electron energy loss spectra of the Allende DM nanodiamond separate. The top spectrum is a sum spectrum from an individual nanodiamond (white box, upper inset). The lower spectrum is a sum spectrum from a region of disordered C (white box, lower inset).

The image intensity can be interpreted quantitatively by use of the $I \propto Z^{1.64}$ relationship established previously (Krivanek et al. 2010), and calibration of the proportionality constant with the quantized variations in the C sheet thickness. Multiple impurity species are present in each sample. The vast majority of the impurities appear to be residual components of the acid dissolution process, e.g., F, Mg, Fe, S, Cl, and Ti, which are physisorbed to the sample surface and mobile under the electron beam. One impurity with an image intensity consistent with Ne was detected in the disordered C phase in the Murchison sample. However, no Xe atoms were observed in either sample. This is consistent with the number of NDs imaged in this study ($\sim 10^3$), and prior analyses of the noble gas and impurity abundances of the Allende DM and other ND separates.

EELS spectra of the C K-edge and plasmon regions were obtained from the NDs and the disordered C phase in each separate. The C K-edge spectrum from a single Allende ND and from a region of disordered C are shown in Figure 4. The ND spectrum is a close match to bulk terrestrial diamond (Egerton 1996), dominated by sp^3 σ^* bonding, with the addition of a small π^* feature at 284.3 eV. The disordered C spectrum has a strong π^* peak, followed by a featureless continuum region that indicates sp^2 π^* bonding without long-range graphitic order. Additional line scan measurements across the diamond-disordered C interface with the ~150 pm probe did not reveal any features, e.g., additional π^* peaks, that suggest ordered surface reconstruction. Thus, the π^* feature in the ND spectrum can be attributed entirely to a layer of disordered C covering the top and bottom surfaces of the ND, without the need to invoke a fullerene-type surface reconstruction or H surface termination (Blake et al. 1988; Garvie 2006).

The low-loss EELS spectra (Figure 5) show two features: a broad peak that shifts in position from ~28 eV on the ND to ~22 eV in the disordered C, and a narrow feature at 4.7 eV in the Murchison separate and 5.6 eV in the Allende

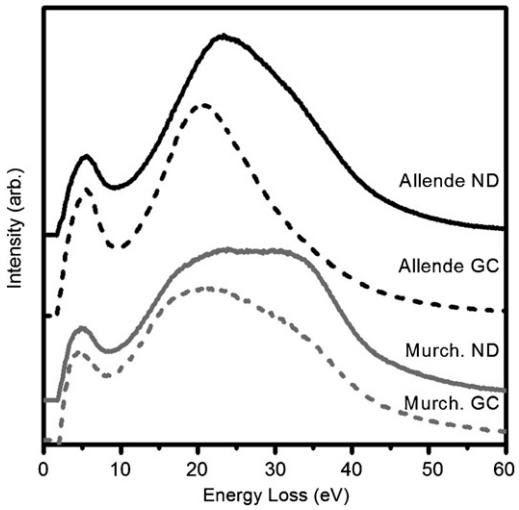

Figure 5. Low-loss electron energy loss spectra of the Allende and Murchison separates.

separate. The broad plasmon peak was previously observed for EELS measurements of the ND separate that averaged over large areas and was attributed to a linear combination of the plasmon feature from the ND interiors and hydrogen terminated surfaces (Bernatowicz et al. 1990). The high spatial-resolution low-loss data in Figure 5 indicate that the broad peak is indeed a superposition of plasmons, but primarily from the ND and spatially distinct disordered C phase, rather than any H termination.

4. DISCUSSION

The terrestrial polytype of C with the most similar properties to the disordered C in the meteoritic ND separates is known as glassy or vitreous C. Distinguishing features of glassy C (GC) include chemical resistance to acids and oxidizers, and sp^2 bonding without long-range graphitic order. Several competing models for the atomic-scale structure of GC have been presented to account for the structural, chemical, and electrical properties. Most recently, Harris (2004) proposed a porous packing of curved C sheet fragments, containing a random packing of 5, 6, and 7 member aromatic rings, in good agreement with our MAADF images of the meteoritic C. Prior studies of the low-loss EELS spectra of GC show plasmon features (Terranova et al. 1996) in good agreement with the disordered C in the ND separates.

Synthetic GC is commonly produced by high temperature treatment of organic materials, including sucrose and phenol resins (Pesin 2002). The typical synthesis temperature range is from 1000°C to 2000°C, although temperatures as low as 600°C and as high as 3000°C have been reported. The presence of non-C species in the organic precursor are believed to favor the formation of GC over graphite. The density and pore structure of GC is a function of the precursor material and heat treatment conditions, but can be as low as 1.3 g/cc. Notably, Lewis et al. (Lewis et al. 1987) reported a density of 2.22–2.33 g/cc for a Murchison ND separate, significantly below the bulk diamond density of 3.51 g/cc, and attributed this to a second phase or radiation-damaged ND. The reduced density compared to bulk diamond can be accounted for if ~50% of the separate is low density GC.

The presence of GC as a major component of the separates has significant implications for the interpretation of results from

prior meteoritic ND studies, for models of ND formation and for interpretation of infrared spectra of the diffuse ISM and some circumstellar envelopes. It is possible that the meteoritic GC and ND are independent phases that formed separately and are found together in the separates by virtue of their shared chemical inertness. However, a recent TEM study of crushed meteorite powders indicate that disordered C is co-located with ND and insoluble organic matter (IOM) in the meteorite matrix (Garvie 2010). This suggests that the formation pathways of the GC, ND, and IOM could be related.

One possible formation scenario relating the GC + ND to IOM is by conversion in the ISM of IOM or its precursors into GC + ND. This scenario can explain the high degree of correlation of the variation in the abundances of ND and IOM in different classes of meteorite (Alexander et al. 2007). It also explains the similarity of the C isotopic compositions of ND separates (Russell et al. 1996) and of IOM to bulk solar system values. The N isotopic compositions of the ND and IOM are different, and thus require more detailed explanation. IOM is isotopically much heavier in N than ND (Alexander et al. 2007) and contains micrometer-sized "hot spots" with $^{15}N/^{14}N$ ratios that are up to four times the terrestrial atmospheric ratio (Busemann et al. 2006), which might result from low temperature (10 K) ion–molecule reactions at the edges of the solar nebula or in dense molecular clouds in the ISM (Rodgers & Charnley 2008). If the ^{15}N enrichment in IOM indeed originates in cold molecular clouds, then the organic precursors of IOM in the diffuse ISM would have lighter N isotopic compositions, more typical of the bulk gas, and thus similar to the GC + ND compositions. If so, conversion of IOM precursors into GC + ND would simply require carbonization by flash heating. If instead the GC + ND formed from ^{15}N-rich IOM, rather than IOM precursors, an additional step of isotopic exchange of N, presumably by back reaction with the bulk ^{14}N-rich gas, would be required. Either process could have occurred by transport of organic material (IOM and/or its precursors) to a region of the ISM that experienced a supernova shockwave.

The GC + ND mixture may result naturally from the partial completion of the carbonization of organics under the high-temperature–high-pressure (HT–HP) conditions induced by a supernova shockwave. Grain–grain and grain–gas collisions induced by supernova winds are thought to be a major mechanism for dust grain destruction in the warm intercloud ISM (Jones et al. 1996) and were also proposed (Tielens et al. 1987) as a mechanism for conversion of amorphous C or graphite into ND. Tielens et al. (1987) specifically argued against the possibility of the conversion of organic molecules into ND, due the difficulty of removing heteroatoms contained in the organics. In contrast, we argue that the heteroatoms contained in organics merely introduce a kinetic barrier that reduces the efficiency of diamond production, while also promoting the polymeric cross linking that stabilizes GC (Pesin 2002). Direct transformation of GC to ND has been demonstrated in laboratory studies (Sumiya et al. 2006) for T $\sim$ 1600°C–2000°C at pressures $\geqslant$15 GPa, which is in good agreement with the conditions achieved during grain–grain collisions in the ISM (Jones et al. 1996). Comparison of the defect microstructure of the meteoritic ND and detonation diamond, produced by shock transformation of TNT and RDX, as well as the relative polytype abundance (cubic diamond versus hexagonal lonsdaleite), has been used to argue in favor of a CVD formation mechanism (Daulton et al. 1996). However, the defect microstructure of ND produced by shock transformation of GC is unknown, and could be closer to the meteoritic ND than that of the synthetic detonation diamond. The ND produced by direct HT–HP transformation of GC is reported to be pure cubic, free of any lonsdaleite (Sumiya et al. 2006).

A supernova shockwave could also result in implantation of noble gas atoms, from both the supernova wind and the ambient ISM gas, into the GC + ND. The relatively low abundance of bona fide supernova isotopic signatures in the GC + ND separates would naturally result from the expected low efficiency of injection of supernova material into the shocked region where the GC + ND is forming. Ion irradiation in the ISM of ND embedded in a graphite-like matrix was previously suggested as an explanation for the He and Ne isotopic compositions of the separates (Huss et al. 2008). More recently, evidence for Si impurity defects in meteoritic ND, which are most easily explained as implanted atoms, rather than growth defects, has been reported (Shiryaev et al. 2011). Furthermore, laboratory studies of ion irradiation of GC with 320 keV Xe^+ ions have shown the production of short-range diamond-like (sp^3) bonding (McCulloch et al. 1994). This suggests that GC can transform to ND during gas–grain collisions by ion irradiation, as well by HT–HP processing.

Although co-formation of GC + ND by a supernova shockwave in the ISM is consistent with the data, it is not the only possible formation scenario. Direct conversion of organic molecules in the ejecta of a type II supernova into GC + ND could also occur, and may be responsible for a minor fraction of the ND separates. However, the bulk C and N isotopic compositions of the separates are inconsistent with the formation of the majority of the separates in a type II supernova. Furthermore, a supernova origin is inconsistent with the high abundance of GC + ND relative to other presolar grains, of which >90% originated in asymptotic giant branch (AGB) and red giant branch (RGB) stars (Alexander 1997).

One prediction of our results is that astronomical observations of ND is likely to occur in association with GC and IOM in the ISM, or with GC in the outflows of type II supernova. Bradley et al. (2005) have shown that organic C and amorphous silicates in interplanetary dust particles have a 5.7 eV feature in their low-loss EELS spectra that matches the 2175 Å extinction feature in the diffuse ISM. The ~5 eV peak we observe in the low-loss EELS spectra of the ND separates is a plausible contributor to this feature as well. Model calculations of the optical properties of NDs encased in GC shells were recently used to reproduce this feature with good agreement (Yastrebov & Smith 2009). The core-shell ND-fullerene structures used in these calculations are similar, but not identical, to the two-phase separates we observe microscopically.

The authors acknowledge support from the Office of Naval Research, NASA, the Materials Science and Technology Division of the Department of Energy, and the Tawani Foundation. R.M.S. thanks G. Duscher for assistance in processing the low-loss EELS data.

REFERENCES

Acke, B., & van den Ancker, M. E. 2006, A&A, 457, 171
Alexander, C. M. O'D. 1997, in AIP Conf. Proc. on Astrophysical Implications of the Laboratory Study of Presolar Materials, ed. T. J. Bernatowicz & E. K. Zinner (Woodbury: AIP), 567
Alexander, C. M. O'D., Fogel, M., Yabuta, H., & Cody, G. D. 2007, Geochim. Cosmochim. Acta, 71, 4380
Bernatowicz, T. J., Gibbons, P. C., & Lewis, R. S. 1990, ApJ, 359, 246

Blake, D. F., Freund, F., Krishnan, K. F. M., et al. 1988, Nature, 332, 611
Bradley, J., Dai, Zu R., Erni, R., et al. 2005, Science, 307, 244
Busemann, H., Young, A. F., Alexander, C. M. O. D., et al. 2006, Science, 312, 727
Clayton, D. D. 1989, ApJ, 340, 613
Dai, Z. R., Bradley, J. P., Joswiak, D. J., et al. 2002, Nature, 418, 157
Daulton, T. L., Eisenhour, D. D., Bernatowicz, T. J., Lewis, R. S., & Buseck, P. R. 1996, Geochim. Cosmochim. Acta, 60, 4853
Egerton, R. F. 1996, Electron Energy-Loss Spectroscopy in the Electron Microscope (2nd ed.; New York: Plenum)
Garvie, L. A. J. 2006, Meteorit. Planet. Sci., 41, 667
Garvie, L. A. J. 2010, in Lunar and Planetary Institute Science Conference Abstracts, LPI Contribution No. 1533, 41,1388
Guillois, O., Ledoux, G., & Reynaud, C. 1999, ApJ, 521, L133
Harris, P. J. F. 2004, Phil. Mag., 84, 3159
Hill, H. G. M., D'Hendecourt, L. B., Perron, C., & Jones, A. P. 1997, Meteorit. Planet. Sci., 32, 713
Huss, G. R., Ott, U., & Koscheev, A. P. 2008, Meteorit. Planet. Sci., 43, 1811
Jones, A. P., Tielens, A. G. G. M., & Hollenbach, D. J. 1996, ApJ, 469, 740
Krivanek, O. L., Chisholm, M. F., Nicolosi, V., et al. 2010, Nature, 464, 571
Lewis, R. S., Huss, G. R., & Lugmair, G. 1991, in Lunar and Planetary Institute Science Conference Abstracts, 22, 807
Lewis, R. S., Ming, T., Wacker, J. F., Anders, E., & Steel, E. 1987, Nature, 326, 160
Maas, R., Loss, R. D., Rosman, K. J. R., et al. 2001, Meteorit. Planet. Sci., 36, 849
McCulloch, D. G., Prawer, S., & Hoffman, A. 1994, Phys. Rev. B, 50, 5905
Pesin, L. A. 2002, J. Mater. Sci., 37, 1
Petrie, S., Stranger, R., & Duley, W. W. 2003, ApJ, 594, 869
Richter, S., Ott, U., & Begemann, F. 1998, Nature, 391, 261
Rodgers, S. D., & Charnley, S. B. 2008, ApJ, 689, 1448
Russell, S. S., Arden, J. W., & Pillinger, C. T. 1996, Meteorit. Planet. Sci., 31, 343
Shiryaev, A. A., Fisenko, A. V., Vlasov, I. I., et al. 2011, Geochim. Cosmochim. Acta, 75, 3155
Sumiya, H., Yusa, H., Inoue, T., Ofuji, H., & Irifune, T. 2006, High Press. Res., 26, 63
Terranova, M. L., Rossi, M., Sessa, V., & Vitali, G. 1996, Phys. Status Solidi a, 154, 127
Tielens, A., Seab, C. G., Hollenbach, D. J., & McKee, C. F. 1987, ApJ, 319, L109
Verchovsky, A. B., Fisenko, A. V., Semjonova, L. F., et al. 2006, ApJ, 651, 481
Yastrebov, S., & Smith, R. 2009, AJ, 697, 1822